the other hand, the evaluation of relative chemiluminescence efficiencies via the correlation of linearized light transients and chronocoulometric data seems firmly based, attractively precise, and applicable to a wide range of systems. It deserves further use.

Particularly intriguing in this work were the effects of the electrolytes on ecl dynamics. Concentrated study of them offers genuine promise for illuminating the elements that control chemiexcitation pathways in condensed phases. New work should be undertaken in that direction.

Contrasting One- and Two-Cation Binding Behavior in *syn*- and *anti*-Anthraquinone Bibracchial Podand (BiP) Mono- and Dianions Assessed by Cyclic Voltammetry and Electron Paramagnetic Resonance Spectroscopy

Milagros Delgado, Deborah A. Gustowski, Hyunsook K. Yoo, Vincent J. Gatto, George W. Gokel,* and Luis Echegoyen*

Contribution from the Department of Chemistry, University of Miami, Coral Gables, Florida 33124. Received June 19, 1987

Abstract: Two new, bibracchial (two-armed) podands (BiPs) based on the anthraquinone ring systems have been prepared. Each has $CH_3O(CH_2CH_2O)_3$ side arms attached in the 1,5 (*anti*-BiP) and 1,8 positions (*syn*-BiP). Reduction of these species either electrochemically or using a reducing metal affords mono- and/or dianions which show significantly different cation affinities depending upon whether or not the side arms are positioned in such a way that cooperation in cation binding may occur. Electron paramagnetic resonance (EPR) results clearly show that reduced *anti*-BiP sequentially binds two cations, obviously from opposite sides, and does so with considerable strength. Remarkably, reduced *syn*-BiP binds two sodium cations as well, apparently on the same side of the anthraquinone residue. Evidence for the latter observation is found in two Na^+ coupling constants of 0.7 G and an increase in total spectral width by nearly a factor of 2. The lithium binding enhancement observed by cyclic voltammetry (0.46 V) with *anti*-BiP is the largest cation binding enhancement yet reported for any switchable lariat ether or podand. Results are compared with a 1,8-anthraquinone-derived crown ether having a total of six oxygen donors in the macroring. Evidence is presented that this crown is an exceptionally strong cation binder not only when reduced (Na^+ coupling constant = 1.43 G), but in its neutral form as well.

The anthraquinone system is an especially interesting one for the study of reducible and switchable lariat ethers[1] because its anion is stable for months in water so long as oxygen is excluded.[2] Although podands (noncyclic polyethylene glycols) generally exhibit poor cation binding,[3] when combined with the semiquinone nucleus, very strong cation complexation is observed for the radical anion.[4] We have recently demonstrated that anthraquinone podands can be used for electrochemically switched cation transport in bulk organic membranes[1d] and have further demonstrated that both monoanion and dianion species can be formed and detected.[1a] In previous work, we have shown that both one- and two-electron reduction can lead to enhanced cation binding in anthraquinone-derived podands and lariat ethers.[1b,c] We have referred to the ability of these systems to exhibit differing cation affinities depending upon whether the radical ion or the dianion is formed as tunability.[1b,c]

We report here our efforts to expand the concept of tunability to include not only the formation of anion and dianion, but the cooperation of these reducible species with one or more side arms adjacent to each other, on opposites sides of the reducible nucleus, and in a macroring. We thus explore the potential for four entries to tunability, namely, one- and two-electron reduction coupled with side-arm and macroring placement. The bulk of the evidence presented here derived from electron paramagnetic resonance studies, so the principal focus of this work is one and/or two cations interacting with the radical anion of anthraquinone (one-electron reduction).

Results and Discussion

Ligand Syntheses. Three substituted anthraquinone derivatives were prepared for the studies reported here. They are shown in Scheme I as **1** (*syn*-BiP), **2** (*anti*-BiP), and **3**. Compounds **1** and **3** were prepared from 1,8-dichloroanthraquinone, and **2** derives from 1,5-dichloroanthraquinone. The podands were prepared by treatment of 1,5- or 1,8-dichloroanthraquinone with the anion (NaH, THF) of $CH_3(OCH_2CH_2)_3OH$. The crown was prepared similarly except that the dianion of tetraethylene glycol was utilized. Details of the procedure for this nucleophilic aromatic substitution reaction are recorded in the Experimental Section.

Dimer crowns, i.e., bis(anthraquinone) crowns, have been previously reported by Akiyama and co-workers.[5] These compounds were prepared by the reaction of 1,8-dihydroxyanthraquinone with mono-, di-, or triethylene glycol ditosylate. This more traditional approach, according to the report,[5] yielded no crowns of the type disclosed here.

(1) (a) Echegoyen, L.; Gustowski, D. A.; Gatto, V. J.; Gokel, G. W. *J. Chem. Soc., Chem. Commun.* **1986**, 220. (b) Gustowski, D. A.; Delgado, M.; Gatto, V. J.; Echegoyen, L.; Gokel, G. W.; *Tetrahedron Lett.* **1986**, 3487 (c) Gustowski, D. A.; Delgado, M.; Gatto, V. J.; Echegoyen, L.; Gokel, G. W.; *J. Am. Chem. Soc.* **1986**, *108*, 7553. (d) Echeverria, L.; Delgado, M.; Gatto, V. J.; Gokel, G. W.; Echegoyen, L.; *Ibid.* **1986**, *108*, 6825.

(2) (a) Stone, E. W.; Maki, A. H. *J. Chem. Phys.* **1962**, *36*, 1944. (b) Stauff, J. *Photochem. Photobiol.* **1965**, *4*, 1199.

(3) (a) Voegtle, F.; Weber, E. *Angew. Chem., Int. Ed. Engl.* **1979**, *18*, 753. (b) Chan, L. L.; Smid, J. *J. Am. Chem. Soc.* **1967**, *89*, 4547. (c) Chan, L. L.; Wong, K. H.; Smid, J. *Ibid.* **1970**, *92*, 1955. (d) Helgeson, R. C.; Weisman, G. R.; Toner, J. L.; Tarnowski, T. L.; Chao, Y.; Mayer, J. M.; Cram, D. J. *Ibid.* **1979**, *101*, 4929.

(4) (a) Bock, H.; Hierholzer, B.; Voegtle, F.; Hollman, G. *Angew. Chem. Int. Ed. Engl.* **1984**, *23*, 57. (b) Wolf, R. E.; Copper, S. R.; *J. Am. Chem. Soc.* **1984**, *106*, 4646. (c) Maruyama, K.; Sohmida, H.; Tsukube, H. *Tetrahedron Lett.* **1985**, *26*, 3583.

(5) Nakatsuji, S.; Ohmori, Y.; Iyoda, M.; Nakashima, K.; Akiyama, S. *Bull. Chem. Soc. Jpn.* **1983**, *56*, 3185.

120   *J. Am. Chem. Soc., Vol. 110, No. 1, 1988*

Delgado et al.

Table I. EPR Coupling Constants for **1**, **2**, and **3**

| compd no. | cation added | coupling constants (G) | | | | | | | LW^a | TSW^b |
		A_1	A_2	A_3	A_4	A_5	A_6	A_M		
1	none^c	1.39	0.52	0.81	1.39	0.52	0.81		0.16	5.44
(*syn*-BIP)	none^c	1.55	0.60	0.84	1.55	0.60	0.84		0.15	5.98
	Li^{+c}	1.14	0.48	1.08	1.14	0.48	1.08		0.20	5.40
	Na$^+$	1.25	0.17	0.95	1.25	0.17	0.95	0.19	0.09	5.31
	2Na$^+$	0.85	0.77	0.77	0.85	0.77	0.77	0.70^d	0.18	8.98
	K$^+$	1.28	0.20	0.91	1.28	0.20	0.91	0.16	0.10	5.26
	2K$^+$	1.52	0.65	0.70	1.52	0.65	0.70		0.38	5.74
2	none	1.20	0.21	1.03	1.20	0.21	1.03		0.10	4.88
anti-BIP	none^c	1.21	0.30	0.99	1.21	0.30	0.99		0.14	5.00
	Li^{+c}	1.21	0.36	1.04	1.21	0.36	1.04		0.14	5.22
	Na$^+$	1.83	0.23	0.79	1.26	0.63	0.69		0.16	5.43
	2Na$^+$	1.26	0.34	0.98	1.26	0.34	0.98		0.16	5.16
	K$^+$	1.75	0.17	0.72	1.33	0.63	0.63		0.21	5.23
	2K$^+$	1.21	0.29	0.98	1.21	0.29	0.98		0.18	5.84
3	none	1.54	0.69	0.69	1.54	0.69	0.69		0.18	5.84
	Li$^+$	1.50		0.71	1.50		0.71	0.19	0.16	4.99
	Na$^+$	1.18	0.23	1.02	1.18	0.23	1.02	1.43	0.18	9.15
	2Na$^+$	1.61	0.74	0.87	1.61	0.74	0.87	1.13	0.49	9.83
	K$^+$	1.17	0.29	1.12	1.17	0.29	1.12		0.20	5.16
	2K$^+$	1.41	0.68	0.78	1.41	0.68	0.78		0.26	5.74

^{a} Line width. ^{b} Total spectral width. ^{c} In CH$_2$Cl$_2$. ^{d} Two equivalent cations.
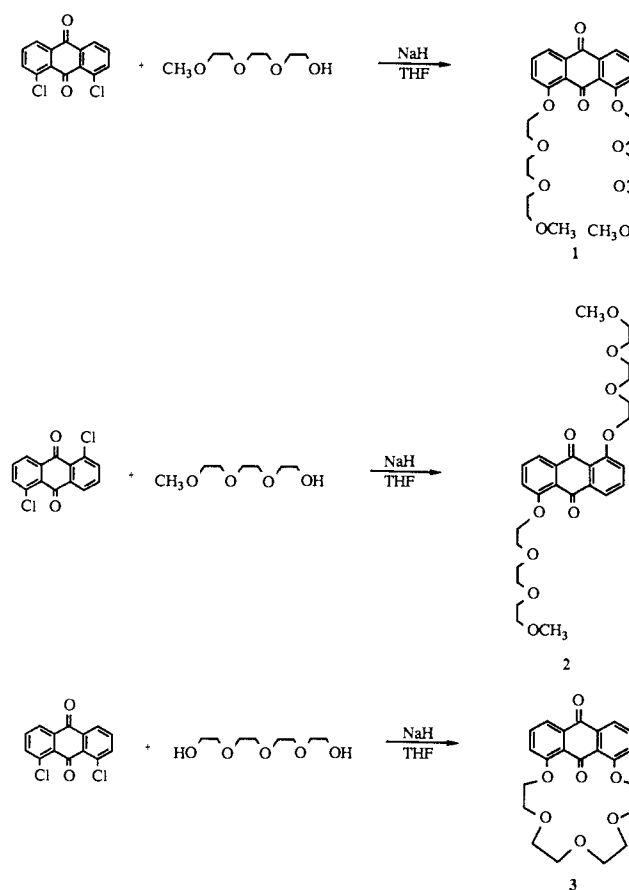
Electron Paramagnetic Resonance Studies. The two side arms were placed on the rigid anthraquione framework in such a way that they could act independently in *anti*-BiP and might cooperate in *syn*-BiP. It was anticipated that *syn*-BiP might bind a single cation very strongly because of the presence of two proximate chains, whereas *anti*-BiP was expected to bind two cations on opposite sides. One question that loomed at the outset was whether two cations might be bound by *anti*-BiP even though it underwent single-electron reduction. It seemed unlikely at the outset that *syn*-BiP would bind two cations, but this surprising behavior is discussed below. The macrocyclic analogue (**3**) was prepared for comparison primarily with *syn*-BiP.

Reduction of these species was effected in either tetrahydrofuran (THF) or CH$_2$Cl$_2$. The preferred solvent was THF but CH$_2$Cl$_2$ was required in one case owing to solubility problems. When THF was used as solvent, reduction was accomplished under high-vacuum conditions using a reducing metal. Thus, the radical anion was produced directly as an ion pair. In order to observe the EPR spectrum of the free species, [2.2.1]- or [2.2.2]cryptand was added to sequester the cation. Electrochemical reduction was done in CH$_2$Cl$_2$ using Bu$_4$NClO$_4$ was supporting electrolyte; this resulted directly in a non-ion-paired species. The metal perchlorate salt was then added to this solution to form the ion pair. Electron paramagnetic resonance spectra were observed using the X-band of an IBM-Bruker ER-200 SRC spectrometer.

EPR Spectra of Reduced *anti*-BiP (2). The EPR spectrum of *anti*-BiP in the absence of alkali metal cations was obtained either in THF or CH$_2$Cl$_2$ as described above. As anticipated, the spectra in these two solvents are similar and exhibit the expected symmetry of three sets of two hydrogens each. The experimentally determined spectrum in THF and the corresponding computer simulation are shown in Figure 1a and 1a', respectively. Minor solvent variations are reflected in the small coupling differences recorded in Table I.

Reduced *anti*-BiP in the Presence of Li$^+$. The influence of Li$^+$ on reduced *anti*-BiP was assessed by cyclic voltammetry and EPR. The cyclic voltammetry results for all of the ligands discussed here are summarized in Table II. We have previously shown[1,6] that the cyclic voltammograms of reducible lariat ethers and podands exhibit the single redox wave expected for the electron acceptor

(6) (a) Kaifer, A.; Echegoyen, L.; Gustowski, D. A.; Goli, D.; Gokel, G. W.; *J. Am. Chem. Soc.* **1983**, *105*, 7168. (b) Gustowski, D. A.; Echegoyen, L.; Goli, D.; Kaifer, A.; Schultz, R. A.; Gokel, G. W. *Ibid.* **1984**, *106*, 1633. (c) Morgan, C. R.; Gustowski, D. A.; Cleary, T. P.; Echegoyen, L.; Gokel, G. W. *J. Org. Chem.* **1984**, *49*, 5008. (d) Kaifer, A.; Gustowski, D. A.; Echegoyen, L.; Gatto, V. J.; Schultz, R. A.; Cleary, T. P.; Morgan, C. R.; Goli, D. M.; Rios, A. M.; Gokel, G. W. *J. Am. Chem. Soc.* **1985**, *107*, 1958. (e) Delgado, M.; Echegoyen, L.; Gatto, V. J.; Gustowski, D. A.; Gokel, G. W. *Ibid.* **1986**, *108*, 4135.

Scheme I

in the absence of cation. When a cation is complexed by both the electron acceptor and the macroring or podand donor groups, a second redox wave is observed at a more positive potential due to ion-pairing. The new potential reflects enhanced cation binding and is shown in Table II as $\Delta E^{1-1'}$. When Li$^+$ is added to a solution of *anti*-BiP, and enhancement of 0.46 V is observed. This is the largest cation-induced binding enhancement we have ever observed with any combination of cation and ligand in any solvent we have studied. As expected, the two-electron reduction of *anti*-BiP is also observed and these data are also recorded in Table II.

The key characteristic of the EPR spectrum of *anti*-BiP in the absence of cation is its symmetry. This symmetry is retained in the presence of Li$^+$ because of the presence of two binding sites

Table II. Anthraquinone Electrochemistry[a]

ligand	M+	equiv	$E_{p(c)}^2$	$E_{p(a)}^2$	$E°^2$	$E_{p(c)}^{2'}$	$E_{p(a)}^{2'}$	$E°^{2'}$	$E_{p(c)}^1$	$E_{p(a)}^1$	$E°^1$	$E_{p(c)}^{1'}$	$E_{p(a)}^{1'}$	$E°^{1'}$	$\Delta E^{2-2'}$	$\Delta E^{1-1'}$
syn-BIP			-1.52	-1.34	-1.43				-1.07	-1.01	-1.04					
	Li+	0.5	-1.53	-1.40	-1.46				-1.07	0.97	-1.02	-0.72	-0.62	-0.67	NO[b]	0.39[c]
		1.0							-1.09	-0.97	-1.03	-0.69	-0.59	-0.64		
		2.0										-0.69	-0.53	-0.61		
	Na+	0.5	-1.42	-1.30	-1.36	-1.34	-1.24	-1.29	-1.06	-1.00	-1.03	-0.92	-0.86	-0.89	0.07	0.14
		1.0				-1.34	-1.20	-1.27				-0.93	-0.83	-0.88		
		2.0				-1.24	-1.11	-1.18				-0.89	-0.80	-0.84		
	K+	0.5	-1.47	-1.30	-1.38				-1.07	-1.00	-1.04	-0.97	-0.90	-0.94	NO	0.10
		1.0	-1.42	-1.29	-1.36				-1.06	-1.00	-1.03	-0.96	-0.90	-0.93		
		2.0	-1.40	-1.29	-1.34				-1.05	-1.00	-1.02	-0.96	-0.90	-0.93		
anti-BiP			-1.48	-1.34	-1.41				-1.06	-1.00	-1.03					
	Li+	0.5	-1.54	-1.35	-1.44				-1.07	-1.00	-1.04	-0.62	-0.54	-0.58	NO	0.46
		1.0							-1.12	-0.99	-1.06	-0.63	-0.52	-0.58		
		2.0										-0.60	-0.50	-0.55		
	Na+	0.5	-1.46	-1.35	-1.40	-1.28	-1.20	-1.24	-1.05	-0.93	-0.99	-0.83	-0.74	-0.78	0.16	0.21
		1.0				-1.22	-1.11	-1.16				-0.82	-0.72	-0.77		
		2.0				-1.23	-1.12	-1.18				-0.78	-0.70	-0.74		
	K+	0.5	-1.44	-1.31	-1.38				-1.05	-0.99	-1.02				NO	NO
		1.0	-1.41	-1.29	-1.35				-1.05	-0.96	-1.00					
		2.0	-1.38	-1.26	-1.32				-1.05	-0.95	-1.00					
3			-1.43	-1.28	-1.36				-1.01	-0.95	-0.98					
	Li+	0.5	-1.47	-1.31	-1.39				-1.01	-0.94	-0.98	-0.61	-0.53	-0.57	NO	0.41
		1.0							-1.00	-0.94	-0.97	-0.60	-0.51	-0.56		
		2.0				— adsorption —										
	Na+	0.5				-1.33[d]	-1.20[d]	-1.26	-1.00	-0.91	-0.96	-0.82	0.71	-0.76	0.10[d]	0.22
		1.0				-1.32[d]	-1.19[d]	-1.26	-1.00	-0.90	-0.95	-0.80	-0.70	-0.75		
		2.0							-0.99	-0.89	-0.94	-0.80	-0.69	-0.74		
	K+	0.5	-1.42	-1.26	-1.34				1.02	-0.90	-0.96	-0.90	-0.78	-0.84	NO	0.14
		1.0	-1.38	-1.26	-1.32				-1.02	-0.92	-0.97	-0.89	-0.78	-0.84		
		2.0	-1.39	-1.26	-1.32							-0.90	-0.78	-0.84		

[a] Potentials are reported vs. SCE. [b] NO means not observed, i.e., no new redox couple was observed. [c] Enhancements are calculated when 0.5 equiv of cation is present and are reported in volts. [d] Shift in the redox potential rather than a new redox couple was observed.
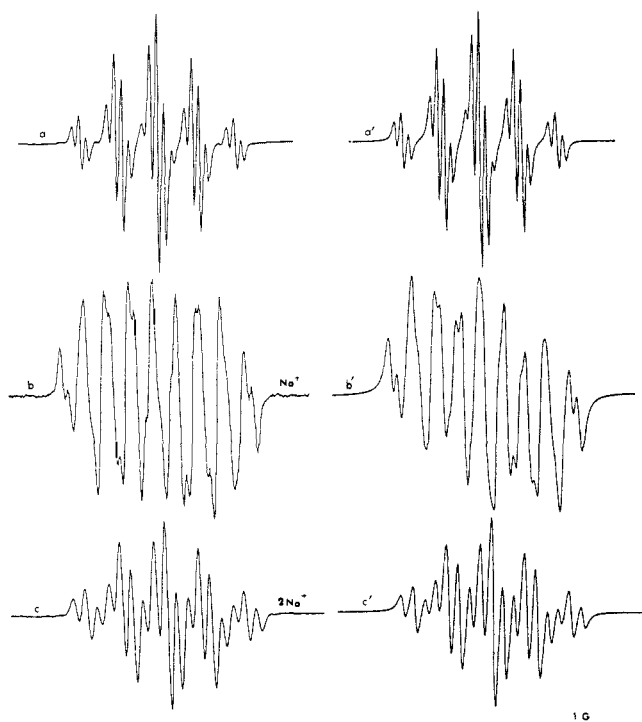

Figure 1. ESR spectra for reduced *anti*-BIP: (a) experimental in THF and (a') simulated; (b) experimental in the presence of 1 equiv of Na+ and (b') simulated; (c) in the presence of 2 equiv of Na+, experimental, and (c') simulated.

interacting with two lithium cations, but only because an excess of Li+ was required when the experiment was conducted in CH₂Cl₂. Solubility problems precluded an examination of the potential single-electron interaction in THF. It is apparent from the data presented in Table I that the coupling constants observed for *anti*-BIP differ only slightly depending upon whether the spectra were observed in THF or CH₂Cl₂. We conclude that ion-pairing and solvation effects are minimal in this case even though such effects are known to occur in other cases.[7]

Reduced *anti*-BiP in the Presence of Na+. Addition of 1 equiv of Na+ to reduced *anti*-BiP in THF affords a spectrum clearly lacking in symmetry (Figure 1b). The best simulation, shown in Figure 1b', was obtained using a different coupling constant for each hydrogen (see Table I). Note that no Na+ splitting is observed. In order to test the possibility of complexation between the anion radical and two metal cations, based on Li+ observations, a second Na+ equivalent was added in the form of its perchlorate. As is obvious from Figure 1c, the second equivalent of Na+ restores the initial high symmetry of the spectrum (i.e., three sets of two hydrogen couplings, Figure 1c'), and, as previously observed for Li+, the values of the coupling constants are very similar to those of the uncomplexed anion radical. This is clear evidence for a 2:1 cation/ligand complex.

Reduced *anti*-BiP in the Presence of K+. The interaction of K+ with the *anti*-BiP radical anion follows the trends observed for Na+. Addition of the first equivalent again results in considerable loss in symmetry. This again suggests complexation of a single K+ on one side of the molecule. Restoration of symmetry results as before from addition of a second equivalent of K+ (Ph₄B⁻ used owing to solubility requirements). Variable-temperature experiments with the samples containing 1 equiv of either Na+ or K+ did not exhibit alternating line-width effects. This strongly suggests a lack of exchange between side chains on opposite sides of the ring, at least within the −10 to +50 °C temperature range studied.

Spectra of *syn*-BiP (1) in the Presence and Absence of Li+. The EPR spectra of all *syn*-BiP species are characterized by high symmetry, in contrast to the situation with *anti*-BiP. All of them were simulated using three sets of two equivalent proton coupling constants (see Table I). In the EPR spectra of *anti*-BiP, no alkali metal coupling constants were resolved. In marked contrast to this, Na+ and K+ coupling constants were not only required for the simulations, their values were substantial, indicating a sig-

(7) Avaca, L. A.; Bewick, A. *Electroanal. Chem. Interfacial Electrochem.* **1973**, *41*, 405. (b) Chauhan, B. G.; Fawcett, W. R.; Lasia, A. *J. Phys. Chem.* **1977**, *81*, 1476. (c) Suga, K.; Aoyagui, S. *Bull. Chem. Soc. Jpn.* **1982**, *55*, 358.

Figure 3. Corey–Pauling–Koltun (CPK) space-filling molecular models showing possible two-cation binding arrangements for the complex *syn*-BiP·Na$^+_2$.

Figure 2. ESR spectra for reduced *syn*-BIP in THF: (a) experimental and (a') simulation; (b) in the presence of 1 equiv of Na$^+$ and (b') simulated; (c) with 2 equiv of Na$^+$ and (c') simulated.

nificant interaction between electron acceptor and cation. Although no Li$^+$ coupling is resolved with *syn*-BIP, the proton coupling constants are strongly perturbed. The Li$^+$ cation interaction clearly occurs on one side of *syn*-BiP whereas the Li$^+$ interaction with *anti*-BiP apparently involves complexation by both carbonyl groups on opposite sides of the anthraquinone nucleus. Although coupling constant differences for *anti*-BiP in THF compared to CH$_2$Cl$_2$ are larger than observed in the *syn*-BiP case, these effects are overwhelmed by addition of Li$^+$ cation. The solvation or ion-pairing interactions with tetrabutylammonium cation known for other systems[7] are therefore negligible in our system.

Reduced *syn*-BiP with Na$^+$. Addition of 1 equiv of Na$^+$ to *syn*-BiP causes a significant change in the proton coupling constants as well, but now a distinct Na$^+$ coupling constant (0.19 G) is observed (see Figure 2, b and b'). Since both podand chains are on the same side of the anthraquinone nucleus, it was anticipated that no or only a small perturbation of the EPR spectrum would result when a second equivalent of Na$^+$ was added. In fact, a remarkable change in the EPR spectrum occurs. The presence of Na$^+$ splitting, arising from two equivalent Na$^+$ cations with a magnitude of 0.7 G, is now observed (see Figure 2c and 2c'). The ring hydrogen coupling constants generally diminish, but the Na$^+$ coupling is so strong that a total line width of 8.98 G is observed compared to 5.44 or 5.31 G in the absence or presence of a single Na$^+$ cation, respectively. For all of the systems thus far described, the typical total line width in either the presence or absence of cation is 5–6 G. Variable-temperature studies (−45 to +65 °C) showed no evidence for line width alternation effects.

All of the evidence above suggests that two Na$^+$ cations are bound by *syn*-BiP. Several obvious structural possibilities present themselves. First, one Na$^+$ may be enveloped by both side arms and a second cation may bind the opposite carbonyl. This seems unlikely since reduced 1-methoxyanthraquinone exhibits no Na$^+$ splitting. Second, the two side arms may form a quasi-planar, pseudo-macroring. The two Na$^+$ cations might then be at opposite apices of a cyclic donor group array. Although we have no direct evidence to discount such a structure, the interaction of one side arm with one Na$^+$ seems intuitively more likely. Such an interaction could occur in two ways. Each side arm could reach about a single cation giving a planar array, or each side arm could
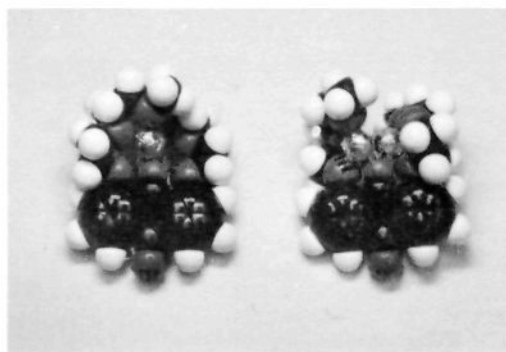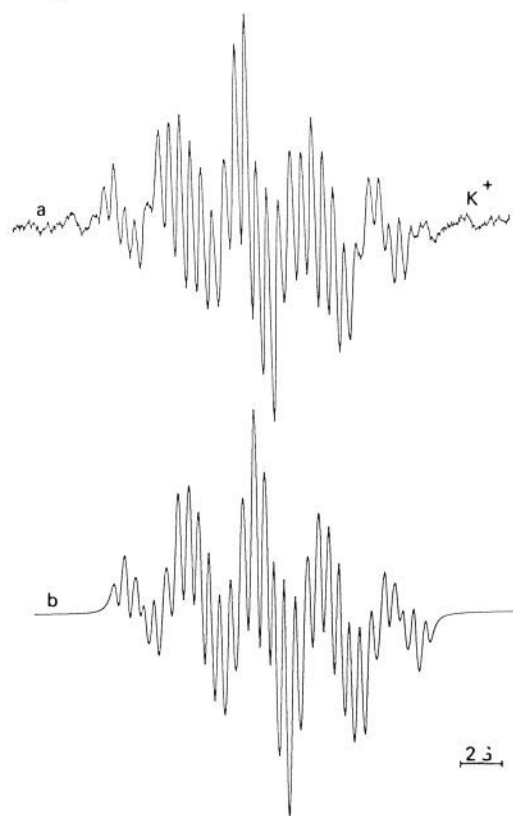

Figure 4. (a) Experimental and (b) simulated ESR spectra for reduced *syn*-BIP in the presence of 1 equiv of K$^+$ in THF.

coil over opposite sides of the anthraquinone residue so that each Na$^+$ is in a nearly tetrahedral environment and both cations share the carbonyl oxygen. The possibilities are depicted in Figure 3.

Based on the models, we favor the latter possibility. We note that coiling such that the two cations and the anthraquinone oxygen are coplanar and perpendicular to the anthraquinone residue is sterically prohibited. We note further that the EPR spectrum of anthraquinone, have a single CH$_3$OCH$_2$CH$_2$OCH$_2$CH$_2$OCH$_2$CH$_2$O side arm in the 1 position, shows, as with *anti*-BIP, no resolved Na$^+$-cation splitting.

Reduced *syn*-BiP with K$^+$. The EPR spectrum of *syn*-BiP in the presence of 1 equiv of K$^+$ is essentially similar to that of *syn*-BiP in the presence of Na$^+$ (Figure 4). A significant difference is that, for the first time in any of our studies,[6,1b,c] a K$^+$ coupling constant (0.16 G) is observed. The total spectral width is also nearly the same as observed for the Na$^+$-*syn*-BiP complex.

When a second equivalent of K$^+$ is added, some changes occur in the proton coupling constants, but the K$^+$ coupling disappears. The line width increases (0.38 vs. 0.10 G), indicating that an exchange process is involved. It is possible that the K$^+$ coupling
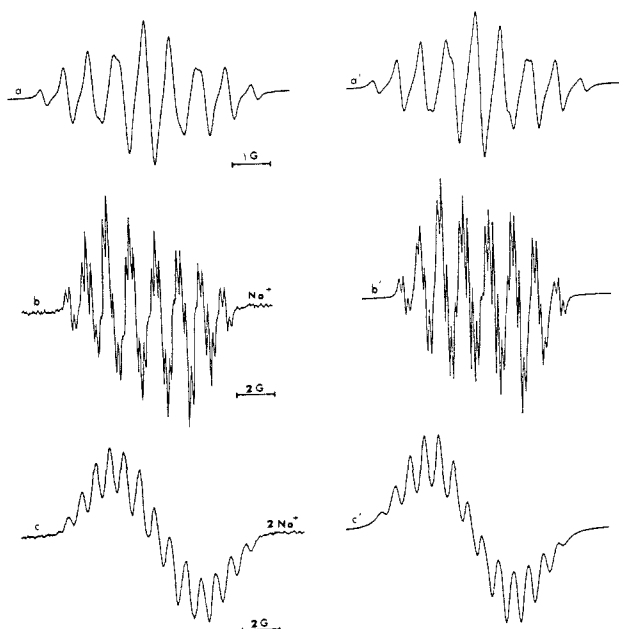
Bibracchial Podands Based on Anthraquinone

J. Am. Chem. Soc., Vol. 110, No. 1, 1988 123

Figure 5. ESR spectra for reduced **3**: (a) experimental in THF and (a′) simulated; (b) experimental in the presence of 1 equiv of Na^+ and (b′) simulated; (c) experimental in the presence of 2 equiv of Na^+ and (c′) simulated.

is unresolved because of this increase in line width. The CV experiments show a very strong K^+ interaction. The presence of the two polyether chains increases the neutral binding (K_1) with K^+. Therefore, there is a sufficient concentration of LK^+ to observe a binding enhancement for the anion radical of 0.10 V.

Reduced Anthraquinone Crown Ether 3. Compound **3** is the analogue of *syn*-BiP and was prepared for comparison purposes. Its EPR spectrum is quite simple as expected for a molecule of this symmetry (see Figure 5a and Table I). Note that coupling constants are presented for only two sets of hydrogens. This is due to accidental degeneracy of two sets of hydrogen coupling constants. The spectral symmetry results from the presence of a C_2 axis containing both carbonyl groups and, presumably, any carbonyl-bound cations.

Reduced 3 with Li^+. Complexation of Li^+ by **3** was studied in THF solution rather than in CH_2Cl_2 as discussed above. As a result, Li^+ was not present in excess. The EPR spectrum in the presence of Li^+ was simulated using a single Li^+ coupling constant of 0.19 G. This value is interesting because we have not previously observed a Li^+ coupling in these systems, but the value is comparable to that previously observed for a related podand system.[1c,d] Only four hydrogen couplings were used in the simulation; the remaining two hydrogen couplings are assumed to be less than 0.16 G (the peak-to-peak line width). The overall spectral width was 4.99 G.

Reduced 3 with Na^+. The remarkable Na^+ splitting, the largest ever reported for a quinone system, is apparent from the spectrum and simulation shown in Figure 5b,b′. The spectrum was simulated using a single Na^+ coupling constant of 1.43 G. The very large Na^+ coupling and the fact that a single Na^+ cation is bound suggest an excellent fit of Na^+ in the macroring cavity. This size correspondence is corroborated by studies of CPK molecular models. An additional indication of this behavior derives from cyclic voltammetric studies of this compound. When a sodium-saturated calomel electrode was used as reference, reproducible results could not be obtained owing to the compound's apparent ability to drain Na^+ from the electrode. Reproducible electrochemical results were obtained only when SSCE was replaced by a silver wire reference electrode. The cation binding enhancement is 0.22 V. This is the largest value for the sodium cation interacting with a reduced anthraquinone ligand obtained thus far.

Another striking feature of the EPR spectrum is that the total spectral width increases from 5.84 G in the absence of any cation to 9.15 G. Although *syn*-BiP shows a comparable increase in

spectral width when Na^+ is present, 2 equiv of cation was present in that case.

Addition of a second equivalent of Na^+ to **3** results in several differences in the EPR spectrum (see Figure 5c). There are some changes in the proton and Na^+ coupling constants. Most noticeable is the attenuation of the Na^+ coupling from 1.43 to 1.13 G. In addition, the total spectral width increases from 9.15 to 9.83 G. Variable-temperature studies (-35 to 65 °C) showed considerable line broadening and some coupling constant modulation effects. This indicates that cation exchange occurs when 2 equiv of Na^+ is present.

The spectrum of $3 \cdot Na^+_2$ was simulated using a single Na^+ coupling constant (1.13 G, see Figure 5c′). This suggests that the key interaction is with one ring-bound cation but that exchange of this cation occurs rapidly on the EPR time scale. The rate of cation exchange must therefore be greater than about 10^8 s^{-1}. This seems unlikely for a three-dimensional, lariat ether-type conformation, because the combination of three-dimensional solvation and increased charge makes these structures rigid. Monocyclic **3** obviously has a higher charge density than the neutral species, but it completely lacks three-dimensionality. The rapid cation exchange thus seems entierly possible and even reasonable with monocyclic **3**.

Reduced 3 with K^+. Because **3** is a fairly rigid molecule and its cavity size is limited, we expected K^+ to be too large to interact strongly. Indeed, the data shown in Table I confirm this. When either 1 or 2 equiv of K^+ is present, the spectra can be simulated using three sets of two hydrogen couplings and no K^+ splitting is observed in either case, but remarkable changes occurred in the spin distribution with the presence of two potassium cations.

Summary

Two podands and a cyclic analogue have been studied by cyclic voltammetric and EPR techniques in the presence and absence of Li^+, Na^+, and K^+ cations. When the two side chains are present on the opposite side (i.e., 1,5) of the anthraquinone residue, the EPR spectrum is symmetrical in the absence of cations. When 1 equiv of either Na^+ or K^+ is present, the spectrum becomes quite unsymmetrical, suggesting that the single cation is bound on one side of the anthraquinone. No cation exchange between carbonyl groups was apparent. When a second equivalent of the same cation was added, symmetry was restored, suggesting that both side arms are involved in complexation. The syn analogue showed a similar EPR spectrum in the absence of cations. When 1 equiv of Na^+ or K^+ is present, the spectrum is clearly perturbed as reflected by Na^+ or K^+ coupling constants. In fact, the K^+ coupling is the first one we have observed in these systems. Addition of a second equivalent of Na^+ leads to an unexpected increase in total spectral width as well as other changes that indicate two Na^+ cations are complexed strongly by reduced **1**. Cyclic analogue (crown ether) **3** shows a large increase in total spectral width when Na^+ is added, mainly as a consequence of a large Na^+ coupling constant of 1.43 G.

Experimental Section

Melting points (Thomas-Hoover apparatus, open capillaries) are uncorrected. Infrared (IR) spectra were recorded on a Perkin-Elmer 281 spectrophotometer as neat samples unless otherwise noted. Spectral bands are reported in cm^{-1} and calibrated against the 1601-cm^{-1} band of polystyrene. Proton nuclear magnetic resonance (^1H NMR) spectra were recorded at 60 MHz as ca 15 wt % solutions in $CDCl_3$ unless otherwise specified. Chemical shifts are reported in parts per million (δ) downfield from internal Me_4Si, and are reported in the order: chemical shift, spin multiplicity (b = broad, s = singlet, d = doublet, t = triplet, q = quartet, m = multiplet), and integration. Combustion analyses (C, H, N) were performed by Atlantic Microlabs, Atlanta, GA.

All reagents were the best grade commercially available and were used without further purification unless otherwise specified. All solvents were distilled prior to use, and tetrahydrofuran (THF) was distilled from CaH_2 or sodium benzophenone. Oven temperatures are given for bulb-to-bulb distillations conducted in a Kugelrohr apparatus. Preparative chromatography columns were packed with Fluka silica gel 60 (70–230 mesh, chromatographic grade). Precoated sheets (silica gel 60 F-254) 0.2 mm thick were used for TLC analyses. Chromatotron chromatography was performed on a Harrison Research Model 7924 Chromatotron using 2-

or 4-mm circular plates prepared from Kieselgel 60 PF-254.

Reagents for Electron Spin Resonance and Cyclic Voltammetry.
Tetrahydrofuran (THF, Aldrich) was flask-to-flask distilled from Na/K
in a vacuum line immediately prior to use. Dichloromethane (Aldrich)
was distilled from CaH_2. All solutions were prepared either under vac-
uum or under an atmosphere of dry N_2. Tetrabutylammonium per-
chlorate (TBAP, Fluka) was twice recrystallized from EtOAc and stored
in a desiccator. Alkali metal perchlorate salts (Aldrich) were recrys-
tallized from deionized water and dried in a vacuum oven at 100 °C for
24 h. Potassium tetraphenylborate (KBPh$_4$) was prepared from sodium
tetraphenylborate (NaBPh$_4$, Aldrich) according to a reported method.[8]
Acetonitrile (Alfa) was distilled from CaH_2 and P_2O_5.

Electron Paramagnetic Resonance. EPR spectra for all cases except
lithium experiments were recorded for dry THF solutions by using the
X-band of an IBM ER-200D SRC spectrometer. Samples were prepared
under vacuum (10^{-3} mm) by reaction of a 10^{-3} M solution of the com-
pound with either sodium or potassium metal as described elsewhere.[9]
The spectra in the absence of metal was obtained by addition of
[2.2.1]cryptand through a break-seal, under vacuum, to the sodium so-
lutions. $NaClO_4$ and KBPh$_4$ were added through a break-seal under
vacuum. Spectra in the presence of Li$^+$ were obtained in purified CH_2Cl_2
by controlled-potential electrolysis by using TBAP as supporting elec-
trolyte and 1 M $LiClO_4$ aqueous solution directly in the ESR cavity. The
potential was controlled between −1.0 and −1.5 V by using a Hewlett-
Packard Model 6200B constant voltage supply.

Cyclic Voltammetry Experiments. The electrochemical experiments
were performed at 25 °C under N_2 in MeCN 0.1 M in TBAP. The
electroactive species was present in millimolar concentrations. Glassy
carbon was used as the working electrode and a Pt wire as the counter
electrode. $E°$ values are reported vs. saturated calomel electrode (SCE).
The measurements were done on a Bioanalytical Systems (Model 100)
electrochemical analyzer, equipped with IR compensation, and recorded
on a Houston DMP-40 plotter.

**1,8-Bis(2-(2-(2-methoxyethoxy)ethoxy)ethoxy)anthracene-9,10-dione,
syn-BIP (1).** A hot solution of 1,8-dichloroanthraquinone (2.0 g, 7.2
mmol) and triethylene glycol monomethyl ether (2.8 g, 17.1 mmol) in
dry THF (30 mL) was slowly added to a vigorously stirred and refluxing
suspension of NaH (60% oil dispersion, 0.9 g, 22.5 mmol) in dry THF
(10 mL) under a nitrogen atmosphere. The reaction mixture was stirred

for 3.5 h, cooled, and concentrated in vacuo. The residue was added to
H_2O (100 mL) and extracted with CH_2Cl_2 (200 mL, then 100 mL). The
combined organic phases were washed with brine (100 mL), dried
($MgSO_4$), and concentrated in vacuo. Column chromatography (silica,
2% MeOH–CH$_2$Cl$_2$) followed by Chromatotron chromatography (silica,
4-mm plate, 2% MeOH–CH$_2$Cl$_2$) gave **1** as a yellow oil (2.44 g, 63.5%):
^{1}H NMR (CDCl$_3$) 3.35 (s, 6 H, OCH$_3$), 3.57–4.38 (m, 24 H,
OCH$_2$CH$_2$O), 7.27–7.88 ppm (m, 6 H, ArH); IR (neat) 2910, 1685,
1605, 1455, 1325, 1295, 1260, 1115 cm^{-1}. Anal. Calcd for $C_{28}H_{36}O_{10}$:
C, 63.13; H, 6.83. Found: C, 63.01; H, 6.87.

**1,5-Bis(2-(2-(2-methoxyethoxy)ethoxy)ethoxy)anthracene-9,10-dione,
anti-BIP (2).** Triethylene glycol monomethyl ether (2.7 g, 16.4 mmol)
was added to a vigorously stirred and refluxing suspension of NaH (60%
oil dispersion, 0.9 g, 22.5 mmol) in dry THF (10 mL) under a nitrogen
atmosphere. After the mixture was stirred for 15 min, 1,5-dichloro-
anthraquinone (2.0 g, 7.2 mmol) in dry THF (30 mL) was added drop-
wise. Workup as for **1** followed
by chromatography (silica, 2% MeOH–CH$_2$Cl$_2$) and Chromatotron
chromatography (silica, 4-mm plate, 2% MeOH–CH$_2$Cl$_2$) gave **2** as a
yellow solid (1.51 g, 39.3%): mp 50.0–51.5 °C; ^{1}H NMR (CDCl$_3$) 3.35
(s, 6 H, OCH$_3$), 3.58–4.39 (m, 24 H, OCH$_2$CH$_2$O), 7.20–7.92 ppm (m,
6 H, ArH); IR (KBr) 2905, 1680, 1605, 1465, 1340, 1290, 1210, 1125
cm^{-1}. Anal. Calcd for $C_{28}H_{36}O_{10}$: C, 63.13; H, 6.83. Found: C, 63.23;
H, 6.85.

1,8-Oxybis(ethyleneoxyethyleneoxy)anthracene-9,10-dione (3). A hot
solution of 1,8-dichloroanthraquinone (4.16 g, 15.0 mmol) and tetra-
ethylene glycol (2.91 g, 15.0 mmol) in dry THF (60 mL) was slowly
added to a vigorously stirred and refluxing suspension of NaH (60% oil
disperion, 1.80 g, 45.0 mmol) in dry THF (20 mL) under a nitrogen
atmosphere. The reaction mixture was stirred for 3.5 h, cooled, and
concentrated in vacuo. The residue was added to H_2O (100 mL) and
extracted with CHCl$_3$ (200 mL, then 100 mL). The combined organic
phases were washed with brine (50 mL), dried ($MgSO_4$), and concen-
trated in vacuo. Column chromatography (100 g of silica gel 60,
CHCl$_3$–2% MeOH/CHCl$_3$) followed by two recrystallization (toluene)
gave 2.7 g (45%) as a yellow crystalline solid: mp 155.0–156.0 °C; ^{1}H
NMR (CDCl$_3$) 3.85–4.32 (m, 16 H, CH$_2$'s), 7.10–7.88 ppm (m, 6 H,
Ar); IR (KBr) 1675, 1590, 1450, 1420, 1890, 1355, 1125, 1075, 755
cm^{-1}. Anal. Calcd for $C_{22}H_{22}O_7$: C, 66.32; H, 5.57. Found: C, 66.21;
H, 5.63.

(8) Bhattacharyya, D. N.; Lee, C. L.; Smid, J.; Szwarc, M. *J. Phys. Chem.*
1965, *69*, 608.

(9) (a) Paul, D. E.; Lipkin, D.; Weissman, S. I. *J. Am. Chem. Soc.* **1956**,
78, 116. (b) Ward, R. L. *Ibid.* **1961**, *83*, 1296. (c) Bolton, J. R.; Fraenkel,
G. K.; *J. Chem. Phys.* **1964**, *40*, 3307.